

Simultaneous State and Parameter Estimation for Second-Order Nonlinear Systems

Rushikesh Kamalapurkar

Abstract—In this paper, a concurrent learning based adaptive observer is developed for a class of second-order nonlinear time-invariant systems with uncertain dynamics. The developed technique results in uniformly ultimately bounded state and parameter estimation errors. As opposed to *persistent* excitation which is required for parameter convergence in traditional adaptive control methods, the developed technique only requires excitation over a finite time interval to achieve parameter convergence. Simulation results in both noise-free and noisy environments are presented to validate the design.

I. INTRODUCTION

Owing to Increasing reliance on automation and increasing complexity of autonomous systems, the ability to adapt has become an indispensable feature of modern control systems. Traditional adaptive control methods (see, e.g., [1]–[3]) attempt to improve the tracking performance, and in general, do not focus on parameter estimation. While accurate parameter estimation can improve robustness and transient performance of adaptive controllers, (see, e.g., [4]–[6]), parameter convergence typically requires restrictive assumptions such as persistence of excitation. An excitation signal is often added to the controller to ensure persistence of excitation; however, the added signal can cause mechanical fatigue and compromise the tracking performance.

Parameter convergence can be achieved under a finite excitation condition using data-driven methods such as concurrent learning (see, e.g., [6]–[8]), where the parameters are estimated by storing data during time-intervals when the system is excited, and then utilizing the stored data to drive adaptation when excitation is unavailable. Concurrent learning has been shown to be an effective tool for adaptive control (see, e.g., [6]–[9]) and adaptive estimation (see, e.g., [10]–[15]), however, concurrent learning typically requires full state feedback along with accurate numerical estimates of the state-derivative.

Novel concurrent learning techniques that can be implemented using full state measurements but without numerical estimates of the state-derivative are developed in [16] and [17]; however, since full state feedback is typically not available, the development of an output-feedback concurrent learning framework is well-motivated. An output feedback concurrent learning technique is developed for second-order linear systems in [18]; however, the implementation critically depends on the certainty equivalence principle, and hence, is not directly transferable to nonlinear systems.

In this paper, an output feedback concurrent learning method is developed for simultaneous state and parameter estimation in second-order uncertain nonlinear systems. An adaptive state-observer is utilized to generate estimates of the state from input-output data. The estimated state trajectories along with the known inputs are then utilized in a novel data-driven parameter estimation scheme to achieve simultaneous state and parameter estimation. Convergence of the state estimates and the parameter estimates to a small neighborhood of the origin is established under a finite (as opposed to *persistent*) excitation condition.

The paper is organized as follows. An integral error system that facilitates parameter estimation is developed in Section II. Section III is dedicated to the design of a robust state observer. Section IV details the developed parameter estimator. Section V details the algorithm for selection and storage of the data that is used to implement concurrent learning. Section VI is dedicated to a Lyapunov-based analysis of the developed technique. Section VII demonstrates the efficacy of the developed method via a numerical simulation and Section VIII concludes the paper.

II. ERROR SYSTEM FOR ESTIMATION

Consider a second order nonlinear system of the form¹

$$\begin{aligned}\dot{p}(t) &= q(t), \\ \dot{q}(t) &= f(x(t), u(t)), \\ y(t) &= p(t),\end{aligned}\tag{1}$$

where $p : \mathbb{R}_{\geq T_0} \rightarrow \mathbb{R}^n$ and $q : \mathbb{R}_{\geq T_0} \rightarrow \mathbb{R}^n$ denote the generalized position states and the generalized velocity states, respectively, $x \triangleq [p^T \ q^T]^T$ is the system state, $f : \mathbb{R}^n \times \mathbb{R}^m \rightarrow \mathbb{R}^n$ is locally Lipschitz continuous, and $y : \mathbb{R}_{\geq T_0} \rightarrow \mathbb{R}^n$ denotes the output. The model f is comprised of a known nominal part and an unknown part, i.e., $f = f^o + g$, where $f^o : \mathbb{R}^n \times \mathbb{R}^m \rightarrow \mathbb{R}^n$ is known and locally Lipschitz and $g : \mathbb{R}^n \times \mathbb{R}^m \rightarrow \mathbb{R}^n$ is unknown and locally Lipschitz. The objective is to design an adaptive estimator to identify the unknown function g , online, using input-output measurements. It is assumed that the system is controlled using a stabilizing input, i.e., $x, u \in \mathcal{L}_\infty$. It is further assumed that the signal p , and u are available for feedback. Systems of the form (1) encompass second-order linear systems and Euler-Lagrange models, and hence, represent a wide class of physical plants, including but not

Rushikesh Kamalapurkar is with the School of Mechanical and Aerospace Engineering, Oklahoma State University, Stillwater, OK, USA. rushikesh.kamalapurkar@okstate.edu.

¹For $a \in \mathbb{R}$, the notation $\mathbb{R}_{\geq a}$ denotes the interval $[a, \infty)$ and the notation $\mathbb{R}_{> a}$ denotes the interval (a, ∞) .

limited to robotic manipulators and autonomous ground, aerial, and underwater vehicles.

Given a compact set $\chi \subset \mathbb{R}^n \times \mathbb{R}^m$, and a constant $\bar{\epsilon}$, the unknown function g can be approximated using basis functions as $g(x, u) = \theta^T \sigma(x, u) + \epsilon(x, u)$, where $\sigma : \mathbb{R}^n \times \mathbb{R}^m \rightarrow \mathbb{R}^p$ and $\epsilon : \mathbb{R}^n \times \mathbb{R}^m \rightarrow \mathbb{R}^n$ denote the basis vector and the approximation error, respectively, $\theta \in \mathbb{R}^{p \times n}$ is a constant matrix of unknown parameters, and there exist $\bar{\sigma}, \bar{\theta} > 0$ such that $\sup_{(x,u) \in \chi} \sigma(x, u) < \bar{\sigma}$, $\sup_{(x,u) \in \chi} \nabla \sigma(x, u) < \bar{\sigma}$, $\sup_{(x,u) \in \chi} \epsilon(x, u) < \bar{\epsilon}$, $\sup_{(x,u) \in \chi} \nabla \epsilon(x, u) < \bar{\epsilon}$, and $\|\theta\| < \bar{\theta}$. To obtain an error signal for parameter identification, the system in (1) is expressed in the form

$$\ddot{q}(t) = f^o(x(t), u(t)) + \theta^T \sigma(x(t), u(t)) + \epsilon(x(t), u(t)). \quad (2)$$

Integrating (2) over the interval $[t - \tau_1, t]$ for some constant $\tau_1 \in \mathbb{R}_{>0}$ and then over the interval $[t - \tau_2, t]$ for some constant $\tau_2 \in \mathbb{R}_{>0}$,

$$\int_{t-\tau_2}^t (q(\lambda) - q(\lambda - \tau_1)) d\lambda = \mathcal{I}f^o(t) + \theta^T \mathcal{I}\sigma(t) + \mathcal{I}\epsilon(t), \quad (3)$$

where \mathcal{I} denotes the integral operator $f \mapsto \int_{t-\tau_2}^t \int_{\lambda-\tau_1}^{\lambda} f(x(\tau), u(\tau)) d\tau d\lambda$. Using the Fundamental Theorem of Calculus and the fact that $q(t) = \dot{p}(t)$, the expression in (4) can be rearranged to form the affine system

$$P(t) = F(t) + \theta^T G(t) + E(t), \quad \forall t \in \mathbb{R}_{\geq T_0} \quad (4)$$

where

$$P(t) \triangleq \begin{cases} p(t - \tau_2 - \tau_1) - p(t - \tau_1) \\ \quad + p(t) - p(t - \tau_2), & t \in [T_0 + \tau_1 + \tau_2, \infty), \\ 0 & t < T_0 + \tau_1 + \tau_2. \end{cases} \quad (5)$$

$$F(t) \triangleq \begin{cases} \mathcal{I}f^o(t), & t \in [T_0 + \tau_1 + \tau_2, \infty), \\ 0, & t < T_0 + \tau_1 + \tau_2, \end{cases} \quad (6)$$

$$G(t) \triangleq \begin{cases} \mathcal{I}\sigma(t), & t \in [T_0 + \tau_1 + \tau_2, \infty), \\ 0 & t < T_0 + \tau_1 + \tau_2, \end{cases} \quad (7)$$

and

$$E(t) \triangleq \begin{cases} \mathcal{I}\epsilon(t), & t \in [T_0 + \tau_1 + \tau_2, \infty), \\ 0 & t < T_0 + \tau_1 + \tau_2. \end{cases} \quad (8)$$

The affine relationship in (4) is valid for all $t \in \mathbb{R}_{\geq T_0}$; however, it provides useful information about the vector θ only after $t \geq T_0 + \tau_1 + \tau_2$.

The knowledge of the generalized velocity, q , is required to compute the matrices F and G . In the following, a robust adaptive velocity estimator is developed to generate estimates of the generalized velocity.

III. VELOCITY ESTIMATOR DESIGN

To generate estimates of the generalized velocity, a velocity estimator inspired by [19] is developed. The estimator is given by

$$\begin{aligned} \dot{\hat{p}} &= \hat{q} \\ \dot{\hat{q}} &= f^o(\hat{x}, u) + \hat{\theta}^T \sigma(\hat{x}, u) + \nu, \end{aligned} \quad (9)$$

where \hat{x} , \hat{p} , \hat{q} , and $\hat{\theta}$ are estimates of x , p , q , and θ , respectively, and ν is a feedback term designed in the following.

To facilitate the design of ν , let $\tilde{p} = p - \hat{p}$, $\tilde{q} = q - \hat{q}$, $\tilde{\theta} = \theta - \hat{\theta}$, and let

$$r(t) = \dot{\tilde{p}}(t) + \alpha \tilde{p}(t) + \eta(t), \quad (10)$$

where the signal η is added to compensate for the fact that the generalized velocity state, q , is not measurable. Based on the subsequent stability analysis, the signal η is designed as the output of the dynamic filter

$$\dot{\eta}(t) = -\beta \eta(t) - kr(t) - \alpha \tilde{q}(t), \quad \eta(T_0) = 0, \quad (11)$$

where α , k , and β are positive constants and the feedback component ν is designed as

$$\nu(t) = \alpha^2 \tilde{p}(t) - (k + \alpha + \beta) \eta(t). \quad (12)$$

The design of the signals η and ν to estimate the state from output measurements is inspired by the p -filter [20]. Using the fact that $\tilde{p}(T_0) = 0$, the signal η can be implemented via the integral form

$$\eta(t) = - \int_{T_0}^t (\beta + k) \eta(\tau) d\tau - \int_{T_0}^t k \alpha \tilde{p}(\tau) d\tau - (k + \alpha) \tilde{p}(t). \quad (13)$$

The affine error system in (4) motivates the adaptive estimation scheme that follows. The design is inspired by the *concurrent learning* technique [21]. Concurrent learning enables parameter convergence in adaptive control by using stored data to update the parameter estimates. Traditionally, adaptive control methods guarantee parameter convergence only if the appropriate PE conditions are met [1, Chapter 4]. Concurrent learning uses stored data to soften the PE condition to an excitation condition over a finite time-interval. Concurrent learning methods such as [6] and [8] require numerical differentiation of the system state, and concurrent learning techniques such as [17] and [16] require full state measurements. In the following, a concurrent learning method that utilizes only the output measurements is developed.

IV. PARAMETER ESTIMATOR DESIGN

To obtain output-feedback concurrent learning update law for the parameter estimates, a history stack, denoted by \mathcal{H} , is utilized. The history stack is a set of ordered pairs $\left\{ (P_i, \hat{F}_i, \hat{G}_i) \right\}_{i=1}^M$ such that

$$P_i = \hat{F}_i + \theta^T \hat{G}_i + \mathcal{E}_i, \quad \forall i \in \{1, \dots, M\}, \quad (14)$$

where \mathcal{E}_i is a constant matrix. If a history stack that satisfies (14) is not available a priori, it is recorded online, based on the relationship in (4), by selecting an increasing set of time-instances $\{t_i\}_{i=1}^M$ and letting

$$P_i = P(t_i), \quad \hat{F}_i = \hat{F}(t_i), \quad \hat{G}_i = \hat{G}(t_i), \quad (15)$$

where

$$\hat{F}(t) \triangleq \begin{cases} \hat{\mathcal{I}} f^o(t), & t \in [T_0 + \tau_1 + \tau_2, \infty), \\ 0, & t < T_0 + \tau_1 + \tau_2, \end{cases} \quad (16)$$

$$\hat{G}(t) \triangleq \begin{cases} \hat{\mathcal{I}} \sigma(t) & t \in [T_0 + \tau_1 + \tau_2, \infty), \\ 0 & t < T_0 + \tau_1 + \tau_2, \end{cases} \quad (17)$$

where $\hat{\mathcal{I}}$ denote the operator $f \mapsto \int_{t-\tau_2}^t \int_{\lambda-\tau_1}^{\lambda} f(\hat{x}(\tau), u(\tau)) d\tau d\lambda$. In this case, the error term \mathcal{E}_i is given by $\mathcal{E}_i = E(t_i) + F(t_i) - \hat{F}(t_i) + \theta^T (G(t_i) - \hat{G}(t_i))$. Let $[t_1, t_2]$ be an interval over which the history stack was recorded. Provided the states and the state estimates remain within a compact set χ over $I \triangleq [t_1 - \tau_1 - \tau_2, t_2]$, the error terms can be bounded as

$$\|\mathcal{E}_i\| \leq L_1 \bar{\epsilon} + L_2 \bar{x}_I, \forall i \in \{1, \dots, M\}, \quad (18)$$

where $\bar{x}_I \triangleq \max_{i \in \{1, \dots, M\}} \sup_{t \in I} \|\hat{x}(t)\|$ and $L_1, L_2 > 0$ are constants.

The concurrent learning update law to estimate the unknown parameters is designed as

$$\dot{\hat{\theta}}(t) = k_\theta \Gamma(t) \sum_{i=1}^M \hat{G}_i (P_i - \hat{F}_i - \hat{\theta}^T(t) \hat{G}_i)^T, \quad (19)$$

where $k_\theta \in \mathbb{R}_{>0}$ is a constant adaptation gain and $\Gamma : \mathbb{R}_{\geq 0} \rightarrow \mathbb{R}^{(2n^2+mn) \times (2n^2+mn)}$ is the least-squares gain updated using the update law

$$\dot{\Gamma}(t) = \beta_1 \Gamma(t) - k_\theta \Gamma(t) \mathcal{G} \Gamma(t). \quad (20)$$

where the matrix $\mathcal{G} \in \mathbb{R}^{p \times p}$ is defined as $\mathcal{G} \triangleq \sum_{i=1}^M \hat{G}_i \hat{G}_i^T$. Using arguments similar to [1, Corollary 4.3.2], it can be shown that provided $\lambda_{\min} \{\Gamma^{-1}(T_0)\} > 0$, the least squares gain matrix satisfies

$$\underline{\Gamma} \mathbf{I}_p \leq \Gamma(t) \leq \bar{\Gamma} \mathbf{I}_p, \quad (21)$$

where $\underline{\Gamma}$ and $\bar{\Gamma}$ are positive constants, and \mathbf{I}_n denotes an $n \times n$ identity matrix.

V. PURGING

The update law in (19) is motivated by the fact that if the full state were available for feedback and if the approximation error, ϵ , were zero, then using $[P_1 \dots P_n]^T = [F_1 \dots F_n]^T + [G_1 \dots G_n]^T \theta$, the parameters could be estimated via the least squares estimate $\hat{\theta}_{LS} = \mathcal{G}^{-1} [G_1 \dots G_n] [P_1 \dots P_n]^T - \mathcal{G}^{-1} [G_1 \dots G_n] [F_1 \dots F_n]^T$. However, since the history stack contains the estimated terms \hat{F} and \hat{G} , during the transient period where the state estimation error is large, the history stack does not accurately (within the

error bound introduced by ϵ) represent the system dynamics. Hence, the history stack needs to be purged whenever better estimates of the state are available.

Since the state estimator exponentially drives the estimation error to a small neighborhood of the origin, a newer estimate of the state can be assumed to be at least as good as an older estimate. A dwell time based greedy purging algorithm is developed in this paper to utilize newer data for estimation while preserving stability of the estimator.

The algorithm maintains two history stacks, a main history stack and a transient history stack, labeled \mathcal{H} and \mathcal{G} , respectively. As soon as the transient history stack is full and sufficient dwell time has passed, the main history stack is emptied and the transient history stack is copied into the main history stack. The sufficient dwell time, denoted by \mathcal{T} , is determined using a Lyapunov-based stability analysis.

Parameter identification in the developed framework imposes the following requirement on the history stack \mathcal{H} .

Definition 1. A history stack $\left\{ (P_i, \hat{F}_i, \hat{G}_i) \right\}_{i=1}^M$ is called full rank if there exists a constant $\underline{c} \in \mathbb{R}$ such that

$$0 < \underline{c} < \lambda_{\min} \{\mathcal{G}\}, \quad (22)$$

where $\lambda_{\min}(\cdot)$ denotes the minimum singular value of a matrix.

Assumption 1. For a given $M \in \mathbb{N}$ and $\underline{c} \in \mathbb{R}_{>0}$, there exists a set of time instances $\{t_i\}_{i=1}^M$ such that a history stack recorded using (15) is full rank.

A singular value maximization algorithm is used to select the time instances $\{t_i\}_{i=1}^M$. That is, a data-point $(P_j, \hat{F}_j, \hat{G}_j)$ in the history stack is replaced with a new data-point $(P^*, \hat{F}^*, \hat{G}^*)$, where $\hat{F}^* = \hat{F}(t)$, $P^* = P(t)$, and $\hat{G}^* = \hat{G}(t)$, for some t , only if

$$s_{\min} \left(\sum_{i \neq j} \hat{G}_i \hat{G}_i^T + \hat{G}_j \hat{G}_j^T \right) < \frac{s_{\min} \left(\sum_{i \neq j} \hat{G}_i \hat{G}_i^T + \hat{G}^* \hat{G}^{*T} \right)}{(1 + \zeta)}, \quad (23)$$

where $s_{\min}(\cdot)$ denotes the minimum singular value of a matrix and ζ is a constant. To simplify the analysis, new data points are assumed to be collected $\tau_1 + \tau_2$ seconds after a purging event. Since the history stack is updated using a singular value maximization algorithm, the matrix \mathcal{G} is a piece-wise constant function of time. The use of singular value maximization to update the history stack implies that once the matrix \mathcal{G} satisfies (22), at some $t = T$, and for some \underline{c} , the condition $\underline{c} < \lambda_{\min}(\mathcal{G}(t))$ holds for all $t \geq T$. The developed purging method is summarized in Fig. 1.

A Lyapunov-based analysis of the parameter and the state estimation errors is presented in the following section.

VI. STABILITY ANALYSIS

Each purging event represents a discontinuous change in the system dynamics; hence, the resulting closed-loop system is a switched system. To facilitate the analysis of the switched system, let $\rho : \mathbb{R}_{\geq 0} \rightarrow \mathbb{N}$ denote a switching signal such

```

1:  $\delta(T_0) \leftarrow 0, \eta(T_0) \leftarrow 0$ 
2: if  $t > \delta(t) + \tau_1 + \tau_2$  and a data point is available then
3:   if  $\mathcal{G}$  is not full then
4:     add the data point to  $\mathcal{G}$ 
5:   else
6:     add the data point to  $\mathcal{G}$  if (23) holds
7:   end if
8:   if  $s_{\min}(\mathcal{G}) \geq \xi \eta(t)$  then
9:     if  $t - \delta(t) \geq \mathcal{T}(t)$  then
10:       $\mathcal{H} \leftarrow \mathcal{G}$  and  $\mathcal{G} \leftarrow 0$   $\triangleright$  purge and replace  $\mathcal{H}$ 
11:       $\delta(t) \leftarrow t$ 
12:      if  $\eta(t) < s_{\min}(\mathcal{G})$  then
13:         $\eta(t) \leftarrow s_{\min}(\mathcal{G})$ 
14:      end if
15:    end if
16:  end if
17: end if

```

Fig. 1. Algorithm for history stack purging with dwell time. At each time instance t , $\delta(t)$ stores the last time instance \mathcal{H} was purged, $\eta(t)$ stores the highest minimum singular value of \mathcal{G} encountered so far, $\mathcal{T}(t)$ denotes the dwell time, and $\xi \in (0, 1]$ denotes a threshold fraction.

that $\rho(0) = 1$, and $\rho(t) = i + 1$, where i denotes the number of times the update $\mathcal{H} \leftarrow \mathcal{G}$ was carried out over the time interval $(0, t)$. For some $s \in \mathbb{N}$, let \mathcal{H}_s denotes the history stack active during the time interval $\{t \mid \rho(t) = s\}$, containing the elements $\left\{ \begin{pmatrix} P_{si}, \hat{F}_{si}, \hat{G}_{si} \end{pmatrix} \right\}_{i=1, \dots, M}$, and let \mathcal{E}_{si}^T be the corresponding error term. To simplify the notation, let $\mathcal{G}_s \triangleq \sum_{i=1}^M \hat{G}_{si} \hat{G}_{si}^T$, and $Q_s = \sum_{i=1}^M \hat{G}_{si} \mathcal{E}_{si}^T$.

Using (14) and (19), the dynamics of the parameter estimation error can be expressed as

$$\dot{\tilde{\theta}}(t) = -k_\theta \Gamma(t) \mathcal{G}_s(t) \tilde{\theta}(t) - k_\theta \Gamma(t) Q_s(t). \quad (24)$$

Since the functions $\mathcal{G}_s : \mathbb{R}_{\geq T_0} \rightarrow \mathbb{R}^{p \times p}$ and $Q_s : \mathbb{R}_{\geq T_0} \rightarrow \mathbb{R}^{p \times n}$ are piece-wise continuous, the trajectories of (24), and of all the subsequent error systems involving \mathcal{G}_s and Q_s , are defined in the sense of Carathéodory. Algorithm 1 ensures that there exists a constant $\underline{g} > 0$ such that $\lambda_{\min}\{\mathcal{G}_s\} \geq \underline{g}$, $\forall s \in \mathbb{N}$.

Using the dynamics in (1), (9) - (11), and the design of the feedback component in (12), the time-derivative of the error signal r is given by

$$\begin{aligned} \dot{r}(t) = & -kr(t) + \tilde{f}^o(x, u, \hat{x}) + \theta^T \tilde{\sigma}(x, u, \hat{x}) - \tilde{\theta}^T \tilde{\sigma}(x, u, \hat{x}) \\ & + \tilde{\theta}^T \sigma(x, u) + \epsilon(x, u) - \alpha^2 \tilde{p} + (k + \alpha) \eta, \end{aligned} \quad (25)$$

where $\tilde{\sigma}(x, u, \hat{x}) = \sigma(x, u) - \sigma(\hat{x}, u)$ and $\tilde{f}^o(x, u, \hat{x}) = f(x, u) - f(\hat{x}, u)$. Since $(x, u) \mapsto f(x, u)$ and $(x, u) \mapsto \sigma(x, u)$ are locally Lipschitz, and since $t \mapsto u(t)$ is bounded, given a compact set $\hat{\chi} \subset \mathbb{R}^n \times \mathbb{R}^m \times \mathbb{R}^n$, there exist $L_f, L_\sigma > 0$ such that $\sup_{(x, u, \hat{x}) \in \hat{\chi}} \|\tilde{f}^o(x, u, \hat{x})\| \leq L_f \|\tilde{x}\|$ and $\sup_{(x, u, \hat{x}) \in \hat{\chi}} \|\tilde{\sigma}(x, u, \hat{x})\| \leq L_\sigma \|\tilde{x}\|$.

To facilitate the analysis, let $\{T_s \in \mathbb{R}_{\geq 0} \mid s \in \mathbb{N}\}$ be a set of switching time instances defined as $T_s = \{t \mid \rho(\tau) < s + 1, \forall \tau \in [0, t) \wedge \rho(\tau) \geq s + 1, \forall \tau \in [t, \infty)\}$.

That is, for a given switching index s , T_s denotes the time instance when the $(s + 1)^{\text{th}}$ subsystem is switched on. The analysis is carried out separately over the time intervals $[T_{s-1}, T_s)$, $s \in \mathbb{N}$, where $T_1 = T_0 + \tau_1 + \tau_2 + t_M$. Since the history stack \mathcal{H} is not updated over the intervals $[T_{s-1}, T_s)$, $s \in \mathbb{N}$, the matrices \mathcal{G}_s and Q_s are constant over each individual interval. The history stack that is active over the interval $[T_s, T_{s+1})$ is denoted by \mathcal{H}_s . To ensure boundedness of the trajectories in the interval $t \in [T_0, T_1)$, the history stack \mathcal{H}_1 is arbitrarily selected to be full rank. The analysis is carried out over the aforementioned intervals using the state vectors $Z \triangleq \begin{bmatrix} \tilde{p}^T & r^T & \eta^T & \text{vec}(\tilde{\theta})^T \end{bmatrix}^T \in \mathbb{R}^{3n+np}$ and $Y \triangleq [\tilde{p}^T \quad r^T \quad \eta^T]^T \in \mathbb{R}^{3n}$ as follows.

Interval 1: First, it is established that Z is bounded over $[T_0, T_1)$, where the bound is $O(\|Z(T_0)\| + \|\sum_{i=1}^M \mathcal{E}_{1i}\| + \bar{\epsilon})$. Given some $\varepsilon > 0$, the bound on Z is utilized to select gains such that $\|Y(T_1)\| < \varepsilon$.

Interval 2: The history stack \mathcal{H}_2 , which is active over $[T_1, T_2)$, is recorded over $[T_0, T_1)$. Without loss of generality, it is assumed that \mathcal{H}_2 represents the system better than \mathcal{H}_1 (which is arbitrarily selected), that is, $\|\sum_{i=1}^M \mathcal{E}_{1i}\| \geq \|\sum_{i=1}^M \mathcal{E}_{2i}\|$. The bound on Z over $[T_1, T_2)$ is then shown to be smaller than that over $[T_0, T_1)$, which utilized to show that $\|Y(t)\| \leq \varepsilon$, for all $t \in [T_1, T_2)$.

Interval 3: Using (18), the errors \mathcal{E}_{3i} are shown to be $O(\|Y_{3i}\| + \bar{\epsilon})$ where Y_{3i} denotes the value of Y at the time when the point $\begin{pmatrix} P_{3i}, \hat{F}_{3i}, \hat{G}_{3i} \end{pmatrix}$ was recorded. Using the facts that the history stack \mathcal{H}_3 , which is active over $[T_2, T_3)$, is recorded over $[T_1, T_2)$ and $\|Y(t)\| \leq \varepsilon$, for all $t \in [T_1, T_2)$, the error $\|\sum_{i=1}^M \mathcal{E}_{3i}\|$ is shown to be $O(\varepsilon + \bar{\epsilon})$. If $T_3 = \infty$ then it is established that $\limsup_{t \rightarrow \infty} \|Z(t)\| = O(\varepsilon + \bar{\epsilon})$. If $T_3 < \infty$ then the fact that the bound on Z over $[T_2, T_3)$ is smaller than that over $[T_1, T_2)$ is utilized to show that $\|Y(t)\| \leq \varepsilon$, for all $t \in [T_2, T_3)$. The analysis is then continued in an inductive argument to show that $\limsup_{t \rightarrow \infty} \|Z(t)\| = O(\varepsilon + \bar{\epsilon})$ and $\|Y(t)\| \leq \varepsilon$, for all $t \in [T_2, \infty)$.

The stability result is summarized in the following theorem.

Theorem 1. Let $\varepsilon > 0$ be given. Let the history stacks \mathcal{H} and \mathcal{G} be populated using the algorithm detailed in Fig. 1. Let the learning gains be selected to satisfy the sufficient gain conditions in (28), (29), (34), and (38). Let $T \in \mathbb{R}_{>0}$ be a time instance such that the system states are exciting over $[T_0, T]$, that is, the history stack can be replenished if purged at any time $t \in [T_0, T]$. Assume that over each switching interval $\{t \mid \rho(t) = s\}$, the dwell-time, \mathcal{T} , is selected such that $\mathcal{T}(t) = \mathcal{T}_s$, where \mathcal{T}_s is selected to be large enough to satisfy (37). Furthermore assume that the

excitation interval is large enough so that $T_2 < T$.² Then, $\limsup_{t \rightarrow \infty} \|Z(t)\| = O(\varepsilon + \bar{\varepsilon})$.

Proof. Provided \mathcal{H}_1 is full rank, then the candidate Lyapunov function

$$2V(Z, t) \triangleq \alpha^2 \tilde{p}^T \tilde{p} + r^T r + \eta^T \eta + \text{tr} \left(\tilde{\theta}^T \Gamma^{-1}(t) \tilde{\theta} \right) \quad (26)$$

can be utilized to establish boundedness of trajectories over $[T_{s-1}, T_s]$. The candidate Lyapunov function satisfies

$$\underline{v} \|Z\|^2 \leq V(Z, t) \leq \bar{v} \|Z\|^2, \quad (27)$$

where $\bar{v} \triangleq \frac{1}{2} \max \{1, \alpha^2, 1/\Gamma\}$ and $\underline{v} \triangleq \frac{1}{2} \min \{1, \alpha^2, 1/\Gamma\}$. The time-derivative of V along the trajectories of (10), (11), (20), (24), and (25) is given by

$$\begin{aligned} \dot{V} = & -\alpha^3 \tilde{p}^T \tilde{p} - kr^T r - \beta \eta^T \eta - \frac{1}{2} \text{tr} \left(\tilde{\theta}^T (k_\theta \mathcal{G}_1 + \beta_1 \Gamma^{-1}) \tilde{\theta} \right) \\ & + r^T \tilde{f}^o + r^T \tilde{\theta}^T \tilde{\sigma} + r^T \tilde{\theta}^T \tilde{\sigma} + r^T \epsilon - k_\theta \text{tr} \left(\tilde{\theta}^T Q_s \right). \end{aligned}$$

Using the Cauchy-Schwartz inequality, the derivative can be bounded as

$$\begin{aligned} \dot{V} \leq & -\alpha^3 \|\tilde{p}\|^2 - k \|r\|^2 - \beta \|\eta\|^2 - \frac{1}{2} \underline{a} \|\tilde{\theta}\|^2 + L_f \|r\| \|\tilde{x}\| \\ & + \|r\| \bar{\theta} L_\sigma \|\tilde{x}\| + \|r\| \|\tilde{\theta}\| \|\tilde{\sigma}\| + \|r\| \bar{\varepsilon} + k_\theta \|\tilde{\theta}\| \bar{Q}_s, \end{aligned}$$

where $\underline{a} = k_\theta \underline{g} + \frac{\beta_1}{\Gamma}$, and \bar{Q}_s is a positive constant such that $\bar{Q}_s \geq \|Q_s\|$. Provided

$$\begin{aligned} k &> \max \left(2(4 + \alpha)(L_f + \bar{\theta} L_\sigma), \frac{12\sigma^2}{\underline{a}} \right), \\ \alpha^3 &> (1 + \alpha)(L_f + \bar{\theta} L_\sigma), \\ \beta &> (L_f + \bar{\theta} L_\sigma), \end{aligned} \quad (28)$$

Young's inequality and nonlinear damping can be used to conclude that

$$\begin{aligned} \dot{V} \leq & -\frac{\alpha^3}{2} \|\tilde{p}\|^2 - \frac{k}{4} \|r\|^2 - \frac{\beta}{2} \|\eta\|^2 - \frac{\underline{a}}{6} \|\tilde{\theta}\|^2 \\ & - \left(\frac{k}{8} - \frac{3L_\sigma}{2\underline{a}} \|\tilde{x}\|^2 \right) \|r\|^2 + \frac{\bar{\varepsilon}^2}{k} + \frac{3k_\theta^2}{2\underline{a}} \bar{Q}_s^2, \end{aligned}$$

Since $\|\tilde{x}\|^2 \leq (1 + \alpha) \|Z\|^2$, $\dot{V} \leq -\nu (\|Z\| - \frac{\iota_s}{\nu})$, in the domain

$$\mathcal{D} \triangleq \left\{ Z \in \mathbb{R}^{3n+np} \mid \|Z\| < \sqrt{\frac{k\underline{a}}{12L_\sigma(1+\alpha)}} \right\}.$$

That is, \dot{V} is negative definite on \mathcal{D} provided $\|Z\| > \sqrt{\frac{\iota_s}{\nu}} > 0$, where $\nu \triangleq \frac{1}{2} \min \{\alpha^3, k/2, \beta, \underline{a}/3\}$ and $\iota_s \triangleq \frac{\bar{\varepsilon}^2}{k} + \frac{3k_\theta^2}{2\underline{a}} \bar{Q}_s^2$. Theorem 4.18 from [22] can then be invoked to conclude that provided

$$k > \frac{15L_\sigma(1+\alpha)}{\underline{a}\nu} \max \left(\bar{V}_s, \frac{\bar{v}\iota_1}{\nu} \right), \quad (29)$$

where $\bar{V}_s \geq \|V(Z(T_{s-1}), T_{s-1})\|$ is a constant, then $\dot{V} \leq -\frac{\nu}{\bar{v}} V + \iota_s$, $\forall t \in [T_{s-1}, T_s]$.

²A minimum of two purges are required to remove the randomly initialized data, and the data recorded during transient phase of the derivative estimator from the history stack.

In particular, $\forall t \in [T_0, T_1]$,

$$V(Z(t), t) \leq \left(\bar{V}_1 - \frac{\bar{v}}{\nu} \right) e^{-\frac{\nu}{\bar{v}}(t-T_0)} + \frac{\bar{v}}{\nu} \iota_1, \quad (30)$$

where $\bar{V}_1 > 0$ is a constant such that $|V(Z(T_0), T_0)| \leq \bar{V}_1$. Hence, $\forall t \in [T_0, T_1]$,

$$\|\tilde{\theta}(t)\| \leq \theta_1 \triangleq \sqrt{\frac{1}{\underline{v}}} \max \left\{ \sqrt{\bar{V}_1}, \sqrt{\frac{\bar{v}}{\nu} \iota_1} \right\}. \quad (31)$$

If it were possible to use the inequality in (30) to conclude that over $[T_0, T_1]$, $V(Z(t), t) \leq V(Z(T_0), T_0)$, then an inductive argument could be used to show that the trajectories decay to a neighborhood of the origin. However, unless the history stack can be selected to have arbitrarily large minimum singular value (which is generally not possible), the constant $\frac{\bar{v}}{\nu} \iota_1$ cannot be made arbitrarily small using the learning gains.

Since ι_s depends on Q_s , it can be made smaller by reducing the estimation errors and thereby reducing the errors associated with the data stored in the history stack. To that end, consider the candidate Lyapunov function

$$W(Y) \triangleq \frac{\alpha^2}{2} \tilde{p}^T \tilde{p} + \frac{1}{2} r^T r + \frac{1}{2} \eta^T \eta. \quad (32)$$

The candidate Lyapunov function satisfies

$$\underline{w} \|Y\|^2 \leq W(Y, t) \leq \bar{w} \|Y\|^2, \quad (33)$$

where $\bar{w} \triangleq \frac{1}{2} \max \{1, \alpha^2\}$, $\underline{w} \triangleq \frac{1}{2} \min \{1, \alpha^2\}$. In the interval $[T_{s-1}, T_s]$, the time-derivative of W is given by

$$\begin{aligned} \dot{W} = & -\alpha^3 \tilde{p}^T \tilde{p} - kr^T r - \beta \eta^T \eta + r^T \left(\tilde{f}^o + (\theta^T - \tilde{\theta}^T) \tilde{\sigma} \right) \\ & + r^T (\tilde{\theta}^T \sigma + \epsilon) \end{aligned}$$

Using the Cauchy-Schwartz inequality, the derivative \dot{W} can be bounded as

$$\begin{aligned} \dot{W} = & -\alpha^3 \|\tilde{p}\|^2 - k \|r\|^2 - \beta \|\eta\|^2 \\ & + (L_f + (\bar{\theta} + \theta_s) L_\sigma) \|r\| \|\tilde{x}\| + (\theta_s \bar{\sigma} + \bar{\varepsilon}) \|r\|, \end{aligned}$$

where $\theta_s > 0$ is a constant such that $\theta_s \geq \sup_{t \in [T_{s-1}, T_s]} \|\tilde{\theta}(t)\|$.

Consider the time interval $[T_0, T_1]$. Provided

$$\begin{aligned} k &\geq 1 + \theta_1^2 + (L_f + (\bar{\theta} + \theta_1) L_\sigma) (4 + \alpha) \\ \alpha^3 &\geq (1 + \alpha) (L_f + (\bar{\theta} + \theta_1) L_\sigma) \\ \beta &\geq (L_f + (\bar{\theta} + \theta_1) L_\sigma) \end{aligned} \quad (34)$$

then $\dot{W} \leq -\frac{w}{\bar{w}} W + \lambda$, where $w = \frac{1}{2} \min \{\alpha^3, k, \beta\}$ and $\lambda = \frac{\bar{\sigma}^2 + \bar{\varepsilon}^2}{2}$. That is, for all $t \in [T_0, T_1]$,

$$W(Y(t), t) \leq \left(\bar{W}_1 - \frac{\bar{w}}{w} \lambda \right) e^{-\frac{w}{\bar{w}}(t-T_0)} + \frac{\bar{w}}{w} \lambda, \quad (35)$$

where $\bar{W}_1 > 0$ is a constant such that $|W(Y(T_0))| \leq \bar{W}_1$. In particular, $\forall t \in [T_0, T_1]$.

$$\|Y(t)\| \leq \sqrt{\frac{1}{\underline{w}}} \max \left(\bar{W}_1, \frac{\bar{w}}{w} \lambda \right) \triangleq \|\bar{Y}\|_1. \quad (36)$$

Provided the dwell time \mathcal{T}_s is large enough so that

$$\begin{aligned} \left(\bar{W}_s - \frac{\bar{w}}{w} \lambda \right) e^{-\frac{w}{\bar{w}} \mathcal{T}_s} &\leq \frac{\bar{w}}{w} \lambda, \\ \left(\bar{V}_s - \frac{\bar{v}}{v} \iota_s \right) e^{-\frac{v}{\bar{v}} \mathcal{T}_s} &\leq \frac{\bar{v}}{v} \iota_s, \end{aligned} \quad (37)$$

then from (30) and (35), $W(Y(T_1)) \leq \frac{2\bar{w}\lambda}{w}$ and $V(Z(T_1), T_1) \leq \frac{2\bar{v}\iota_1}{v}$. In particular, $\|Y(T_1)\| \leq \sqrt{\frac{2\bar{w}\lambda}{ww}}$ and $\|Z(T_1)\| \leq \sqrt{\frac{2\bar{v}\iota_1}{vv}}$. Note that the bound on $Y(T_1)$ can be made arbitrarily small by increasing k , α , and β .

Now the interval $[T_1, T_2)$ is considered. Since the history stack \mathcal{H}_2 which is active during $[T_1, T_2)$ is recorded during $[T_0, T_1)$, the bound in (18) can be used to show that $\bar{Q}_2 = O(\|Y\|_1 + \bar{\epsilon})$.

Since \mathcal{H}_1 is independent of the system trajectories, \bar{Q}_1 can be selected such that $\bar{Q}_2 < \bar{Q}_1$, and hence, $\iota_2 < \iota_1$. Thus, provided the constant \bar{V}_1 (and as a result, the gain k) is selected large enough so that

$$\frac{2\bar{v}\iota_1}{v} < \bar{V}_1, \quad (38)$$

the gain condition in (29) holds over $[T_1, T_2)$, and hence, a similar Lyapunov-based analysis, along with the bound $\bar{V}_2 = \frac{2\bar{v}\iota_1}{v}$ can be utilized to conclude that $\forall t \in [T_1, T_2)$,

$$\|\tilde{\theta}(t)\| \leq \sqrt{\frac{\bar{v}}{vv}} \max\{\sqrt{2\iota_1}, \sqrt{\iota_2}\} \triangleq \theta_2. \quad (39)$$

The sufficient condition in (38) implies that $\bar{V}_2 < \bar{V}_1$ and hence, (31) and $\iota_2 < \iota_1$ imply that $\theta_2 < \theta_1$.

Since $\theta_2 < \theta_1$, the gain conditions in (34) hold over the interval $[T_1, T_2)$. A Lyapunov-based analysis similar to (32)-(36) yields $\|Y(t)\| \leq \sqrt{\frac{1}{w} \max(\bar{W}_2, \frac{\bar{w}}{w} \lambda)}$. From (37), $\bar{W}_2 = \frac{2\bar{w}\lambda}{w}$, and hence, $\forall t \in [T_1, T_2)$,

$$\|Y(t)\| \leq \sqrt{\frac{2\bar{w}\lambda}{ww}} \triangleq \|Y\|_2. \quad (40)$$

Now, the interval $[T_2, T_3)$ is considered. Since the history stack \mathcal{H}_3 which is active during $[T_2, T_3)$ is recorded during $[T_1, T_2)$, the bounds in (18) and (40) can be used to show that $\bar{Q}_3 = O(\|Y\|_2 + \bar{\epsilon})$. By selecting \bar{W}_1 large enough, it can be ensured that $\|Y\|_2 < \|Y\|_1$, and hence, $\bar{Q}_3 < \bar{Q}_2$, which implies $\iota_3 < \iota_2$. Provided \mathcal{T}_2 satisfies (37), then $(\bar{V}_2 - \frac{\bar{v}}{v} \iota_2) e^{-\frac{v}{\bar{v}} (T_2 - T_1)} \leq \frac{\bar{v}}{v} \iota_2$, which implies $\bar{V}_3 = \frac{\bar{v}}{v} \iota_2$, and hence, $\bar{V}_3 < \bar{V}_2$ and $\theta_3 < \theta_2$. Therefore, the gain conditions in (28), (29), and (34) are satisfied over $[T_2, T_3)$.

Since the gain conditions are satisfied, a Lyapunov-based analysis similar to (32)-(36) yields $\|Y(t)\| \leq \sqrt{\frac{2\bar{w}\lambda}{ww}}, \forall t \in [T_2, T_3)$. Given any $\varepsilon > 0$, the gains α , β , and k can be selected large enough to satisfy $\|Y\|_2 \leq \varepsilon$, and hence, $\|Y(t)\| \leq \varepsilon, \forall t \in [T_2, T_3)$. Furthermore, a similar Lyapunov-based analysis as (26) - (30) yields $V(Z(t), t) \leq (\bar{V}_3 - \frac{\bar{v}}{v} \iota_3) e^{-\frac{v}{\bar{v}} (t - T_2)} + \frac{\bar{v}}{v} \iota_3, \forall t \in [T_2, T_3)$. If $T_3 = \infty$ then $\limsup_{t \rightarrow \infty} V(Z(t), t) \leq \frac{\bar{v}}{v} \iota_3$, which, from

TABLE I
SIMULATION PARAMETERS FOR THE DIFFERENT SIMULATION RUNS.
THE PARAMETERS ARE SELECTED USING TRIAL AND ERROR.

Parameter	Noise Variance	
	0	0.001
T_1	0.5	0.9
T_2	0.3	0.5
N	50	150
$\Gamma(t_0)$	I_4	I_4
β_1	0.5	0.5
α	2	2
k	10	10
β	2	2
ζ	0	0
ξ	0.95	0.95
k_θ	0.5N	0.5N

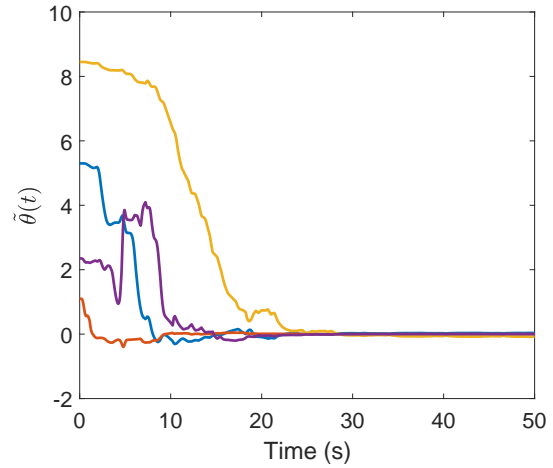


Fig. 2. Trajectories of the parameter estimation errors using noise-free position measurements.

$\bar{Q}_3 = O(\|Y\|_2 + \bar{\epsilon})$ and $\iota_3 = \frac{\bar{\epsilon}^2}{k} + \frac{3k_\theta^2}{2a} \bar{Q}_3^2$ implies that $\limsup_{t \rightarrow \infty} \|Z(t)\| = O(\varepsilon + \bar{\epsilon})$.

If $T_3 \neq \infty$ then an inductive continuation of the Lyapunov-based analysis to the time intervals $[T_{s-1}, T_s)$ shows that provided the dwell time \mathcal{T}_s satisfies (37), the gain conditions in (28), (29), and (34) are satisfied for all $t > T_3$, the state Y satisfies

$$\|Y(t)\| \leq \varepsilon, \forall t > T_1, \quad (41)$$

and $Q_s \leq Q_{s-1}$, $\iota_s \leq \iota_{s-1}$, $\bar{V}_s \leq \bar{V}_{s-1}$, and $\bar{\theta}_s \leq \bar{\theta}_{s-1}$, for all $s > 3$.

The bound in (41) and the fact that $\bar{Q}_s = O(\|Y\|_{s-1} + \bar{\epsilon})$ indicate that $\bar{Q}_s = O(\varepsilon + \bar{\epsilon}), \forall s \in \mathbb{N}$. Furthermore, $V(Z(t), t) \leq (\bar{V}_s - \frac{\bar{v}}{v} \iota_s) e^{-\frac{v}{\bar{v}} (t - T_{s-1})} + \frac{\bar{v}}{v} \iota_s, \forall t \in [T_{s-1}, T_s), \forall s \in \mathbb{N}$, which, along with the dwell time requirement, implies that $\limsup_{t \rightarrow \infty} V(Z(t), t) \leq \frac{\bar{v}}{v} \iota_s$, and hence, $\limsup_{t \rightarrow \infty} \|Z(t)\| = O(\varepsilon + \bar{\epsilon})$. \square

VII. SIMULATION

The developed technique is simulated using a model for a two-link robot manipulator arm. The uncertainty $g(x, u)$ is linearly parameterizable as $g^T(x, u) = \theta^T \sigma(x, u)$. That

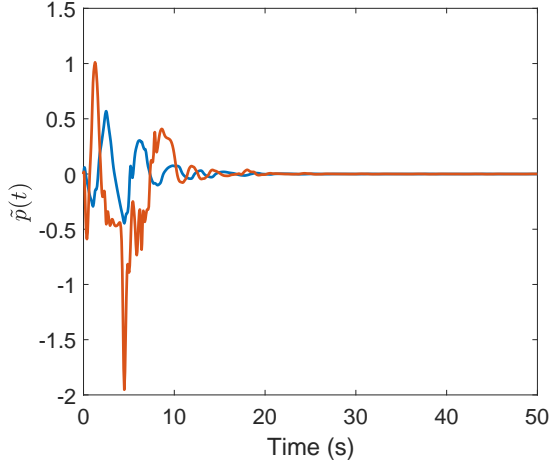


Fig. 3. Trajectories of the generalized position estimation errors using noise-free position measurements.

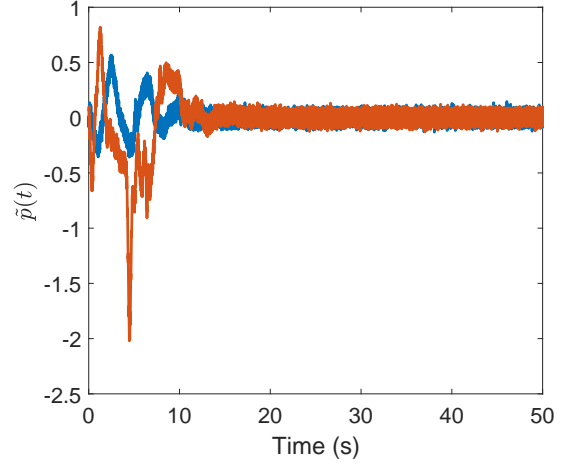


Fig. 6. Trajectories of the generalized position estimation errors with a Gaussian measurement noise (variance = 0.001).

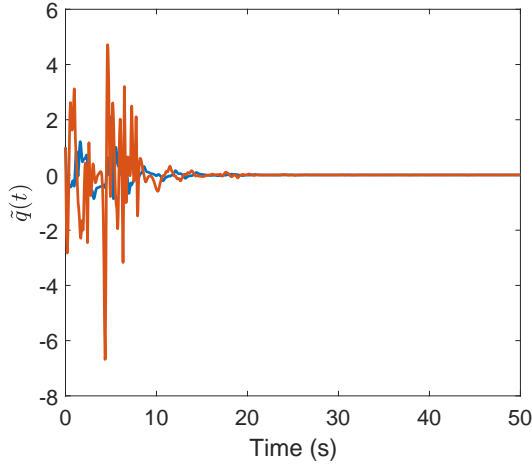


Fig. 4. Trajectories of the generalized velocity estimation errors using noise-free position measurements.

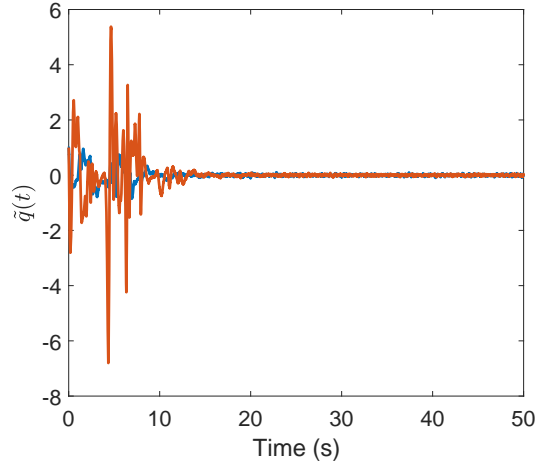


Fig. 7. Trajectories of the generalized velocity estimation errors with a Gaussian measurement noise (variance = 0.001).

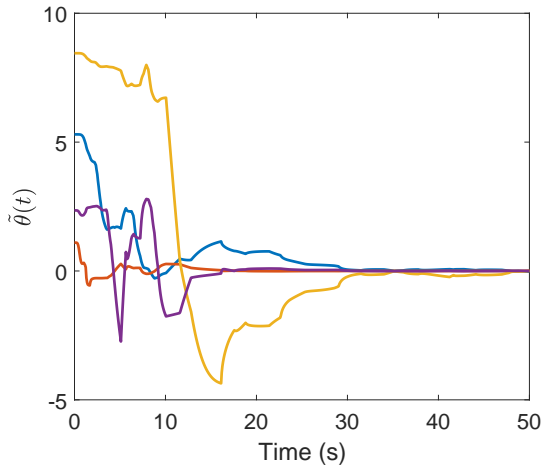


Fig. 5. Trajectories of the parameter estimation errors with a Gaussian measurement noise (variance = 0.001).

is, the selected model belongs to a sub-class of systems defined by (1), where the function approximation error, ε , is zero. Since the ideal parameters, θ , are uniquely known, the selected model facilitates quantitative analysis of the parameter estimation error. The dynamics of the arm are described by (1), where

$$\begin{aligned} f^0(x, u) &= -(M(p))^{-1} V_m(p, q) q + (M(p))^{-1} u, \\ g^T(x, u) &= \theta^T \begin{bmatrix} (M(p))^{-1} & (M(p))^{-1} \end{bmatrix} D(q)^T. \end{aligned} \quad (42)$$

In (42), $u \in \mathbb{R}^2$ is the control input, $D(q) \triangleq \text{diag}[\tanh(q_1), \tanh(q_2)]$, $M(p) \triangleq \begin{bmatrix} p_1 + 2a_3c_2(p) & a_2 + a_3c_2(p) \\ a_2 + a_3c_2(p) & a_2 \end{bmatrix}$, and $V_m(p, q) \triangleq \begin{bmatrix} -a_3s_2(p)q_2 & -a_3s_2(p)(q_1 + q_2) \\ a_3s_2(p)q_1 & 0 \end{bmatrix}$, where $c_2(p) = \cos(p_2)$, $s_2(p) = \sin(p_2)$, and $a_1 = 3.473$, $a_2 = 0.196$, and $a_3 = 0.242$ are constants. The system has four unknown

parameters. The ideal values of the unknown parameters are $\theta = [5.3 \ 1.1 \ 8.45 \ 2.35]^T$.

The contribution of this paper is the design of a parameter estimator and a velocity observer. The controller is assumed to be any controller that results in bounded system response. In this simulation study, the controller, u , is designed so that the system tracks the trajectory $p_1(t) = p_2(t) = \sin(3t) + \sin(2t)$.

The simulation is performed using Euler forward numerical integration using a sample time of $T_s = 0.0005$ seconds. Past $\frac{\tau_1 + \tau_2}{T_s}$ values of the generalized position, p , and the control input, u , are stored in a buffer. The matrices P , \hat{G} , and \hat{F} for the parameter update law in (19) are computed using trapezoidal integration of the data stored in the aforementioned buffer. Values of P , \hat{G} , and \hat{F} are stored in the history stack and are updated according to the algorithm detailed in Fig. 1.

The initial estimates of the unknown parameters are selected to be zero, and the history stack is initialized so that all the elements of the history stack are zero. Data is added to the history stack using a singular value maximization algorithm. To demonstrate the utility of the developed method, three simulation runs are performed. In the first run, the observer is assumed to have access to noise free measurements of the generalized position. In the second run, a zero-mean Gaussian noise with variance 0.001 is added to the generalized position signal to simulate measurement noise. The values of various simulation parameters selected for the three runs are provided in Table I. Figure 2 demonstrates that in absence of noise, the developed parameter estimator drives the state estimation error, \tilde{x} , and the parameter estimation error, $\tilde{\theta}$, close to the origin. Figures 5 - 7 indicate that the developed technique can be utilized in the presence of measurement noise, with expected degradation of performance.

VIII. CONCLUSION

This paper develops a concurrent learning based adaptive observer and parameter estimator to simultaneously estimate the unknown parameters and the generalized velocity of second-order nonlinear systems using generalized position measurements. The developed technique utilizes a dynamic velocity observer to generate state estimates necessary for data-driven adaptation. A purging algorithm is developed to improve the quality of the stored data as the state estimates converge to the true state. By integrating n -times, the developed method can be generalized to higher-order linear systems.

Simulation results indicate that the developed method is robust to measurement noise. A theoretical analysis of the developed method under measurement noise and process noise is a subject for future research. Future efforts will also focus on the examination the effect of the integration intervals, τ_1 and τ_2 , on the performance of the developed estimator.

REFERENCES

[1] P. Ioannou and J. Sun, *Robust Adaptive Control*. Prentice Hall, 1996.

[2] S. Sastry and M. Bodson, *Adaptive Control: Stability, Convergence, and Robustness*. Upper Saddle River, NJ: Prentice-Hall, 1989.

[3] M. Krstić, I. Kanellakopoulos, and P. V. Kokotović, *Nonlinear and Adaptive Control Design*. New York, NY, USA: John Wiley & Sons, 1995.

[4] M. A. Duarte and K. Narendra, "Combined direct and indirect approach to adaptive control," *IEEE Trans. Autom. Control*, vol. 34, no. 10, pp. 1071–1075, Oct 1989.

[5] M. Krstić, P. V. Kokotović, and I. Kanellakopoulos, "Transient-performance improvement with a new class of adaptive controllers," *Syst. Control Lett.*, vol. 21, no. 6, pp. 451–461, 1993.

[6] G. Chowdhary and E. Johnson, "A singular value maximizing data recording algorithm for concurrent learning," in *Proc. Am. Control Conf.*, 2011, pp. 3547–3552.

[7] G. Chowdhary, T. Yucelen, M. Mühlegg, and E. N. Johnson, "Concurrent learning adaptive control of linear systems with exponentially convergent bounds," *Int. J. Adapt. Control Signal Process.*, vol. 27, no. 4, pp. 280–301, 2013.

[8] S. Kersting and M. Buss, "Concurrent learning adaptive identification of piecewise affine systems," in *Proc. IEEE Conf. Decis. Control*, Dec. 2014, pp. 3930–3935.

[9] G. Chowdhary, M. Mühlegg, J. How, and F. Holzapfel, "Concurrent learning adaptive model predictive control," in *Advances in Aerospace Guidance, Navigation and Control*, Q. Chu, B. Mulder, D. Choukroun, E.-J. van Kampen, C. de Visser, and G. Looye, Eds. Springer Berlin Heidelberg, 2013, pp. 29–47.

[10] H. Modares, F. L. Lewis, and M.-B. Naghibi-Sistani, "Integral reinforcement learning and experience replay for adaptive optimal control of partially-unknown constrained-input continuous-time systems," *Automatica*, vol. 50, no. 1, pp. 193–202, 2014.

[11] R. Kamalapurkar, J. Klotz, and W. E. Dixon, "Concurrent learning-based online approximate feedback Nash equilibrium solution of N -player nonzero-sum differential games," *IEEE/CAA J. Autom. Sin.*, vol. 1, no. 3, pp. 239–247, Jul. 2014, Special Issue on Extensions of Reinforcement Learning and Adaptive Control.

[12] B. Luo, H.-N. Wu, T. Huang, and D. Liu, "Data-based approximate policy iteration for affine nonlinear continuous-time optimal control design," *Automatica*, 2014.

[13] R. Kamalapurkar, P. Walters, and W. E. Dixon, "Model-based reinforcement learning for approximate optimal regulation," *Automatica*, vol. 64, pp. 94–104, Feb. 2016.

[14] T. Bian and Z.-P. Jiang, "Value iteration and adaptive dynamic programming for data-driven adaptive optimal control design," *Automatica*, vol. 71, pp. 348–360, 2016.

[15] R. Kamalapurkar, J. A. Rosenfeld, and W. E. Dixon, "Efficient model-based reinforcement learning for approximate online optimal control," *Automatica*, vol. 74, pp. 247–258, Dec. 2016.

[16] R. Kamalapurkar, B. Reish, G. Chowdhary, and W. E. Dixon, "Concurrent learning for parameter estimation using dynamic state-derivative estimators," *IEEE Trans. Autom. Control*, 2017, to appear.

[17] A. Parikh, R. Kamalapurkar, and W. E. Dixon, "Integral concurrent learning: Adaptive control with parameter convergence without PE or state derivatives," 2017, submitted, see arXiv:1512.03464, *Automatica*.

[18] R. Kamalapurkar, "Online output-feedback parameter and state estimation for second order linear systems," in *Proc. Am. Control Conf.*, 2017, to appear, see also, arXiv:1609.05879.

[19] H. T. Dinh, R. Kamalapurkar, S. Bhasin, and W. E. Dixon, "Dynamic neural network-based robust observers for uncertain nonlinear systems," *Neural Netw.*, vol. 60, pp. 44–52, Dec. 2014.

[20] B. Xian, M. S. de Queiroz, D. M. Dawson, and M. McIntyre, "A discontinuous output feedback controller and velocity observer for nonlinear mechanical systems," *Automatica*, vol. 40, no. 4, pp. 695–700, 2004.

[21] G. Chowdhary, "Concurrent learning for convergence in adaptive control without persistency of excitation," Ph.D. dissertation, Georgia Institute of Technology, Dec. 2010.

[22] H. K. Khalil, *Nonlinear Systems*, 3rd ed. Upper Saddle River, NJ: Prentice Hall, 2002.